Supporting Information

Enwrapping graphdiyne (g-C_nH_{2n-2}) on hollow $NiCo_2O_4$ nanocages derived from Prussian blue analogue as a p-n heterojunction for highly efficient photocatalytic hydrogen evolution

Haiyan Xie, Kai Wang*, Dingzhou Xiang, Songling Li, Zhiliang Jin*

School of Chemistry and Chemical Engineering, Ningxia Key Laboratory of Solar Chemical Conversion Technology, Key Laboratory for Chemical Engineering and Technology, State Ethnic Affairs Commission, North Minzu University, Yinchuan 750021, P.R.China

Corresponding author: kaiwang@nun.edu.cn (K.W.); zl-jin@nun.edu.cn (Z. L. Jin).

1. Experimental details Supplement

1.1 Characterization

The phase structure of the powder samples was examined on an X-ray diffractometer (XRD, CuKα radiation, λ = 1.5405 Å). The molecular structures of the materials were analyzed by Fourier transform infrared (FTIR-650) spectroscopy and Raman spectroscopy (Raman, USA-Thermo Fisher Dxr 2Xi). The morphology and microstructure of all samples were documented using a scanning electron microscope (SEM, S4800FE-SEM) and a transmission electron microscope (TEM, JEM1200EX-JEOL). The surface elemental composition of the samples and the chemical valence states present were analyzed using a radiation photoelectron spectrometer (XPS, 300 W Al Kα). The nitrogen adsorption-desorption isotherms of the samples were measured using an ASAP 2460M nitrogen adsorber at 77 K. The optical absorption properties of the samples in the wavelength range of 200 ~ 800 nm were investigated using a UV-Vis absorption spectrometer (UV-Vis, PerkinElmer Lamda-750) equipped with a spectrophotometer. A fluorescence spectrophotometer (F-7000, Japan) was used to produce the photoluminescence emission spectra (PL) and time-resolved photoluminescence (TRPL) spectra at an excitation wavelength of 480 nm. Density functional theory (DFT) calculation is based on the Dmol3 model in generalized gradient approximation (GGA) and Perdew-Burke-Ernzerhof (PBE) to study the density of states of catalysts.

1.2 Photoelectrochemical measurements

An electrochemical workstation (AMETEK, VersaSTAT4-400) was used for photoelectrochemical experiments. Specifically, catalyst powder was prepared by depositing catalyst powder on a pre-prepared conductive glass as the working electrode, and the saturated glyceryl electrode and Pt electrode were used as the references, respectively. A 300 W xenon lamp as the light source and 0.2 M Na_2SO_4 solution as the electrolyte. At an open-circuit voltage of 0.2 V, transient photocurrent curves (IT) and electrochemical impedance spectra (EIS) were produced. By linear scanning voltammetry (LSV), the polarization curves of the samples were recorded with a variation of 0.2 V vs. SCE. Mott-Schottky test measurements were performed at -1.0 ~ 1.0 V vs. SCE bias at 500, 1000, and 1500 Hz, respectively.

1.3 Photocatalytic hydrogen evolution experiments

All photocatalytic reactions were performed in a closed system using a 50 mL quartz vial. First,

10 mg of pre-prepared catalyst and a certain amount of EY were dispersed in 30 mL of triethanolamine (TEOA) solution. The suspension of the catalyst was sonicated until uniformly dispersed and degassed with nitrogen for 5 min. Subsequently, it was placed in a nine-channel photocatalytic reaction system equipped with a 5W LED for the reaction and the quantity of hydrogen precipitation was measured with a gas chromatograph (Tianmei GC7900, N_2 as carrier). The AQE was calculated according to the following equation.

$$\mathrm{AQE} = \frac{2 \times \text{the number of evolved hydrogen molecules}}{\text{the number of incident photons}} \times 100\%$$

2. Supporting Figs. and Tables

Scheme S1. Proposed mechanism for the synthesis of graphdiyne (GDY).

Fig. S1. XRD patterns of (a) (x)$NiCo_2O_4$@GDY (x=10, 20, 30, 40, 50, 60) samples.

Fig. S2. Raman spectra of GDY samples.

Fig. S3. Full survey XPS spectrum of (a) GDY, (b) $NiCo_2O_4$ and $NiCo_2O_4$@GDY.

Table S1. Comparison of GDY-based composites for photocatalytic H_2 production.

Fig. S4. XRD of $NiCo_2O_4$@GDY before and after four PHE cycles.

Fig. S5. High-resolution XPS of (a) Ni 2p, (b) Co 2p, (c) O 1s and (d) C 1s in $NiCo_2O_4$@GDY before and after four PHE cycles.

Fig. S6. Cyclic voltammograms (0-0.2 V vs. SCE) recorded at different scanning rates (40-80 mV/s) in 0.2 M Na_2SO_4 solution for (a) GDY, (b) $NiCo_2O_4$, and (c) $NiCo_2O_4$@GDY; (d) The relationship of the as-synthesized catalysts between current density variation and scan rate fitted to a linear regression allows for the estimation of Cdl.

Fig. S7. PL spectral changes at a different time under illumination in a mixed solution with TA (0.5 mM) and NaOH (2 mM) of (a)GDY, (b) $NiCo_2O_4$, (c) $NiCo_2O_4$@GDYsamples; (d) The concentration of hydroxyl radicals for different samples against irradiation time.

Fig. S8. A p-n heterojunction mechanism towards the charge transfer between GDY and $NiCo_2O_4$ before contact and after contact in darkness and under illumination.

Fig. S9. An amorphous/crystalline system of $NiCo_2O_4$@GDY.

Fig. S10. Hollow structure of $NiCo_2O_4$ $NiCo_2O_4$@GDY.

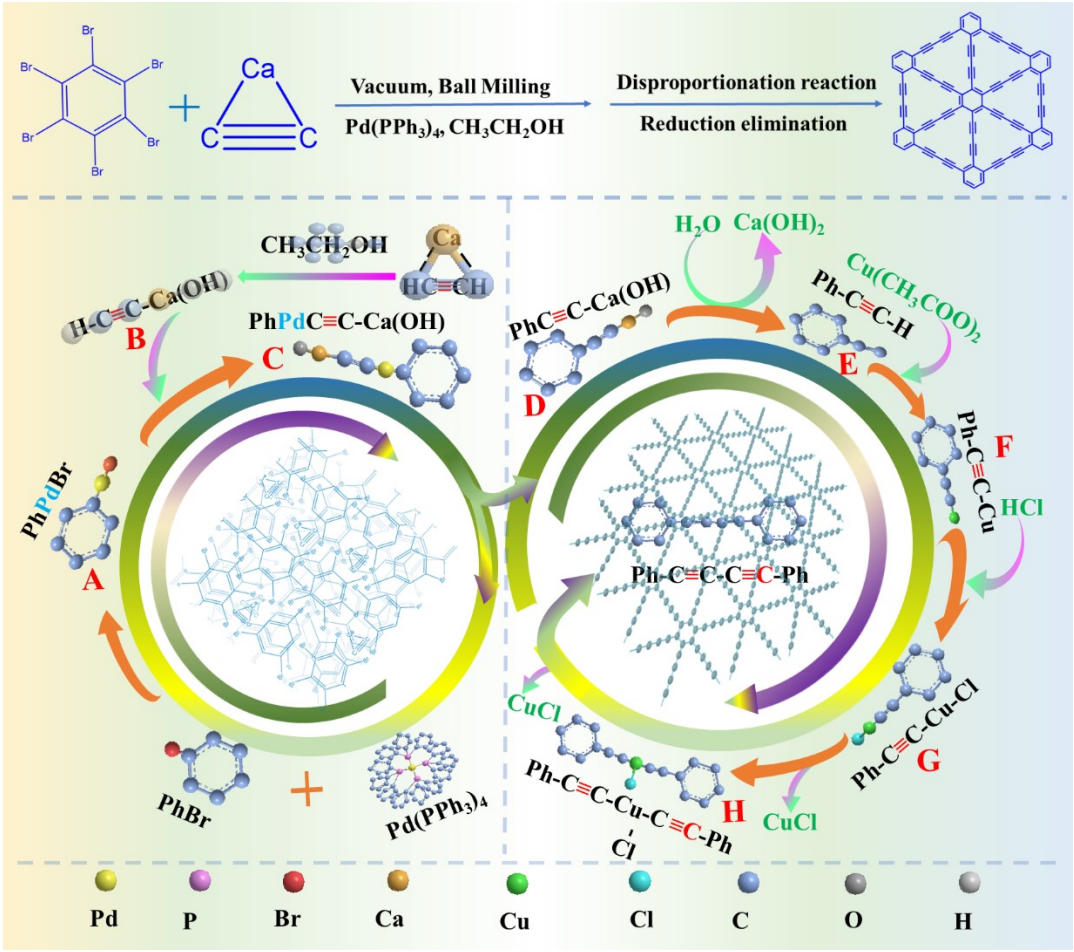

Scheme S1. Proposed mechanism for the synthesis of graphdiyne (GDY).

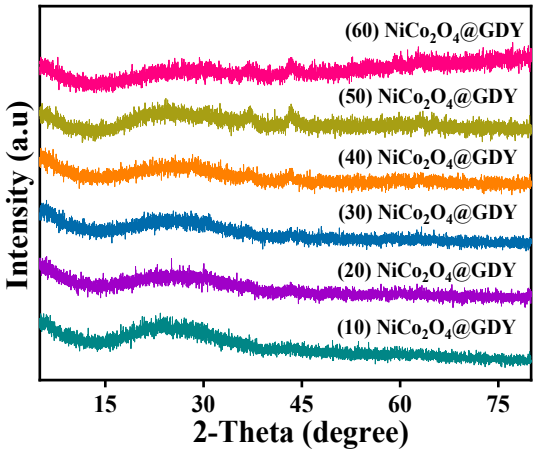

Fig. S1. XRD patterns of (a) (x)$NiCo_2O_4$@GDY (x=10, 20, 30, 40, 50, 60) samples.

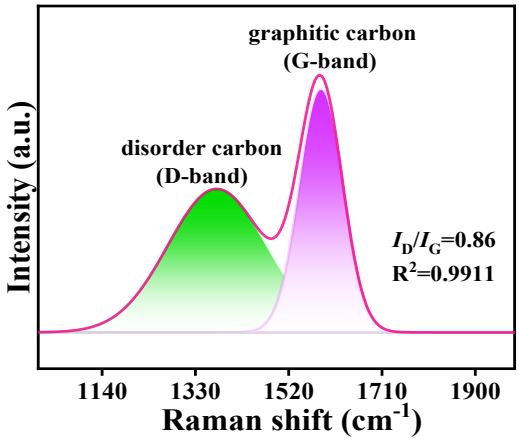

Fig. S2. Raman spectra of GDY samples.

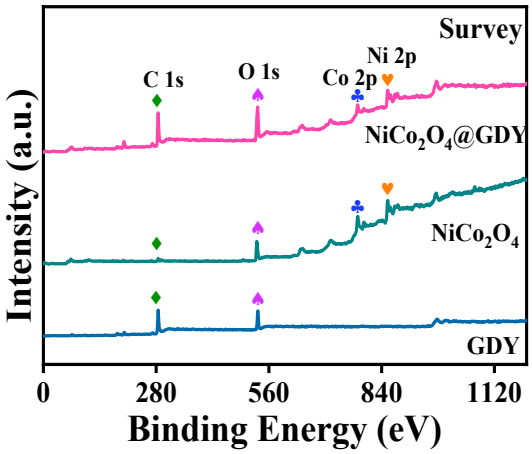

Fig. S3. Full survey XPS spectrum of (a) GDY, (b) $NiCo_2O_4$ and $NiCo_2O_4$@GDY.

Table S1. Comparison of GDY-based composites for photocatalytic H_2 production.

Photocatalysts	Light sources	Sacrificial reagent	Activity ($mmol \cdot g^{-1} \cdot h^{-1}$)	Ref.
$NiCo_2O_4$/GDY	5 W LED	15% TEOA	4.84	**This work**
GDY@g-C_3N_4/Pt	100 W xenon lamp	15% TEOA	3.25	[S1]
GDY/CuI/Co-S-P	5 W LED	15% TEOA	2.71	[S2]
NiBi/GDY	300 W xenon lamp	25% Methanol	2.27	[S3]
g-C_3N_4/Co_3S_4@S, N-GDY	5 W LED	15% TEOA	2.07	[S4]
GDY/CuBr	5 W LED	15% TEOA	1.45	[S5]
Co_9S_8/GDY/CuI	5 W LED	15% TEOA	1.41	[S6]
GDY/CuI/NiO	5 W LED	15% TEOA	1.19	[S7]
GDY/NiS	5 W LED	15% TEOA	0.82	[S8]

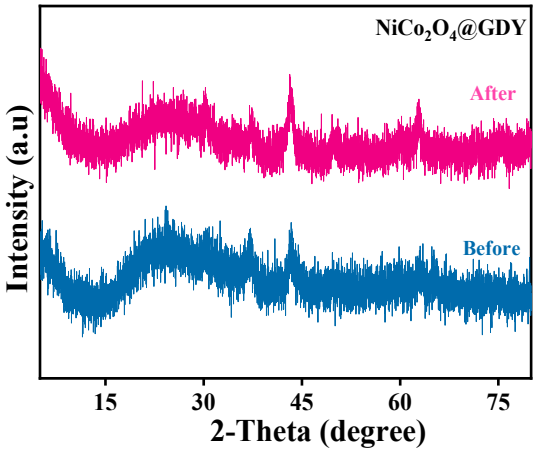

Fig. S4. XRD of $NiCo_2O_4$@GDY before and after four PHE cycles.

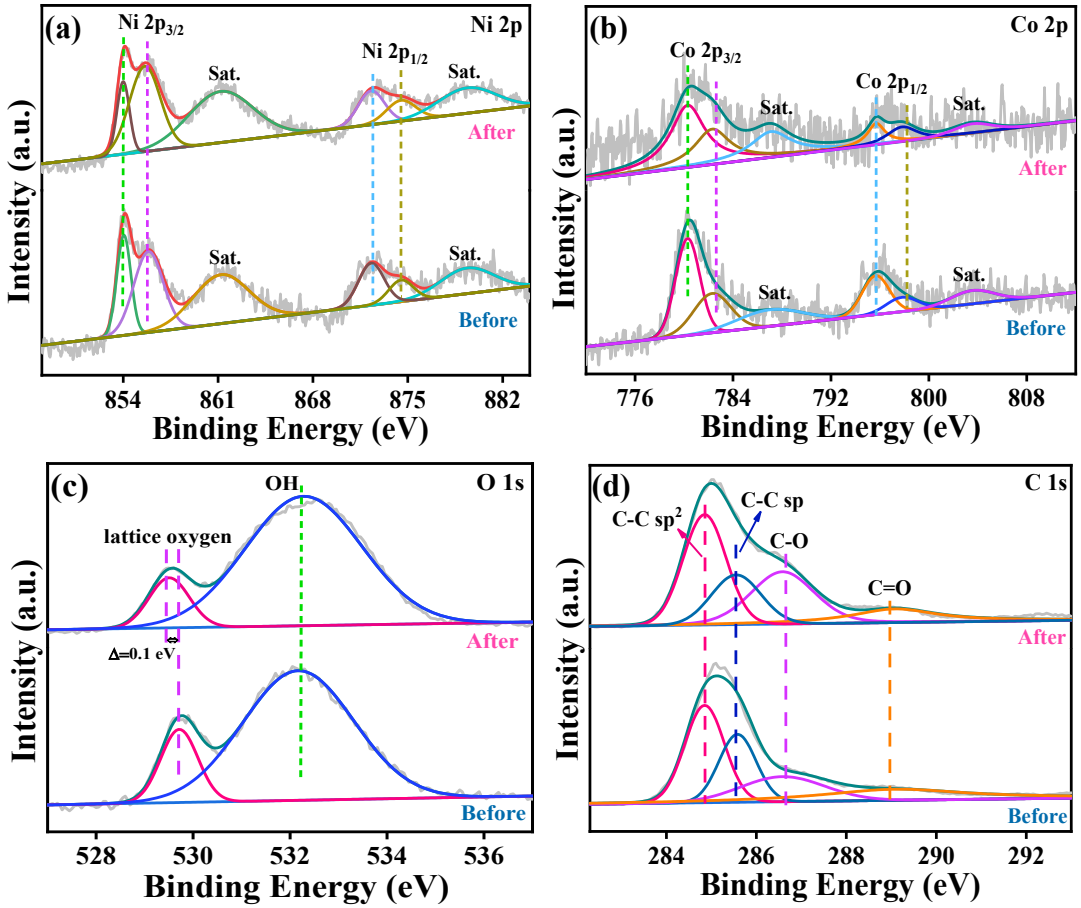

Fig. S5. High-resolution XPS of (a) Ni 2p, (b) Co 2p, (c) O 1s and (d) C 1s in $NiCo_2O_4$@GDY before and after four PHE cycles.

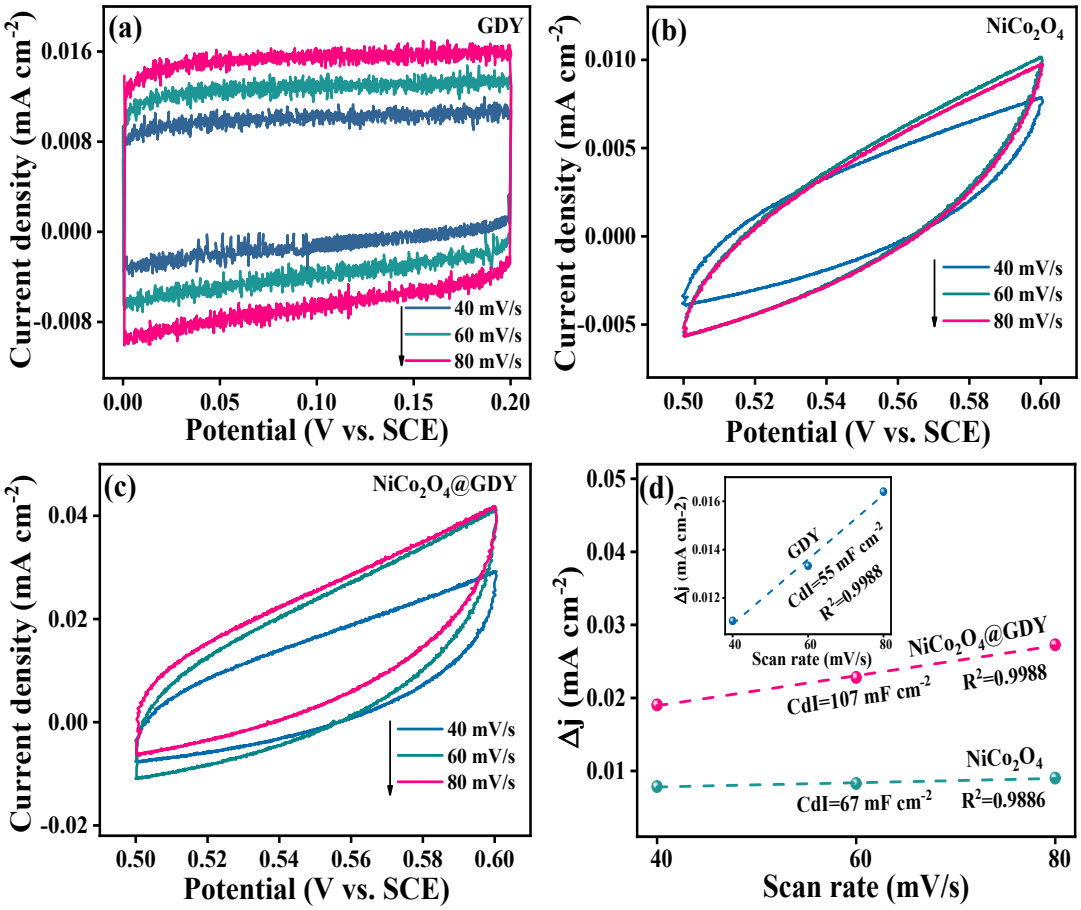

Fig. S6. Cyclic voltammograms (0-0.2 V vs. SCE) recorded at different scanning rates (40-80 mV/s) in 0.2 M Na_2SO_4 solution for (a) GDY, (b) $NiCo_2O_4$, and (c) $NiCo_2O_4$@GDY; (d) The relationship of the as-synthesized catalysts between current density variation and scan rate fitted to a linear regression allows for the estimation of Cdl.

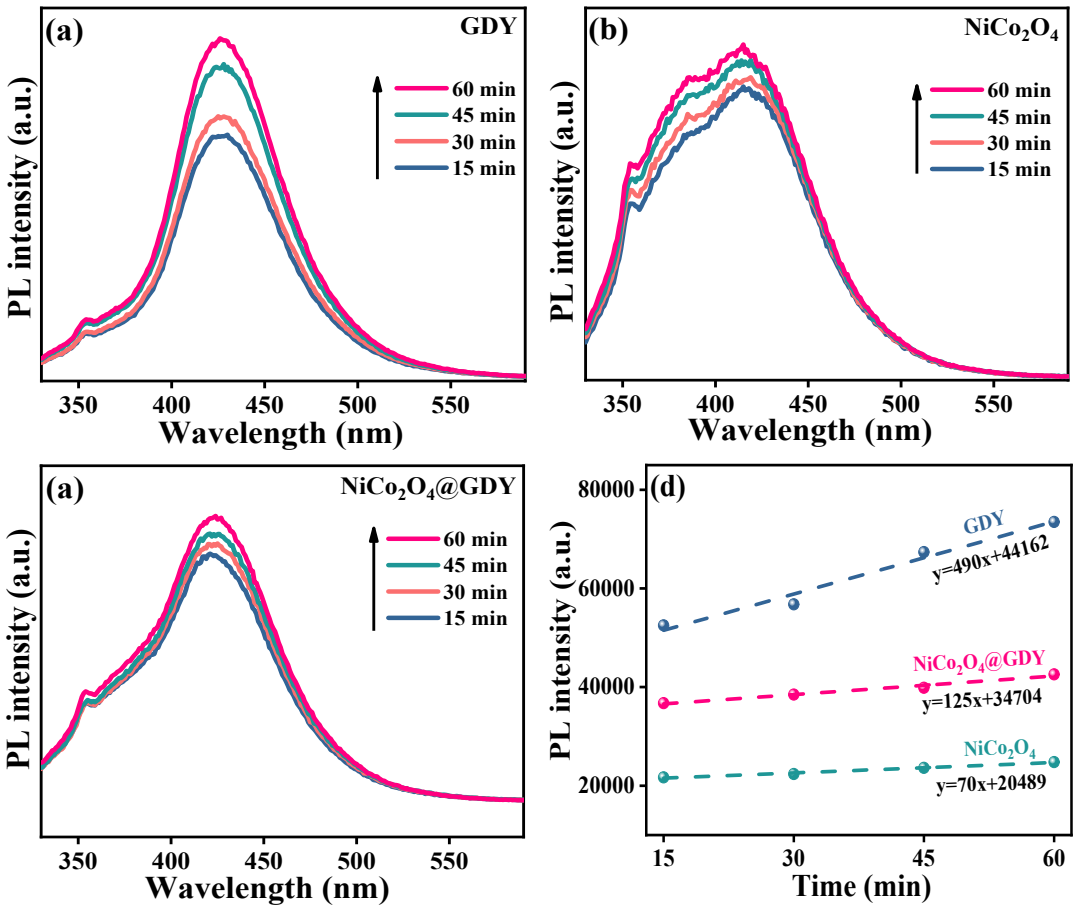

Fig. S7. PL spectral changes at a different time under illumination in a mixed solution with TA (0.5 mM) and NaOH (2 mM) of (a)GDY, (b) $NiCo_2O_4$, (c) $NiCo_2O_4$@GDYsamples; (d) The concentration of hydroxyl radicals for different samples against irradiation time.

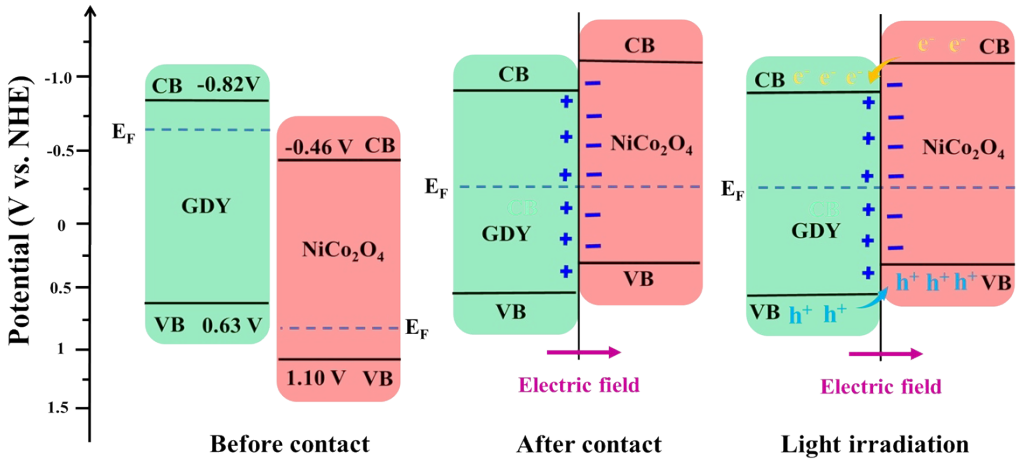

Fig. S8. A p-n heterojunction mechanism towards the charge transfer between GDY and $NiCo_2O_4$ before contact and after contact in darkness and under illumination.

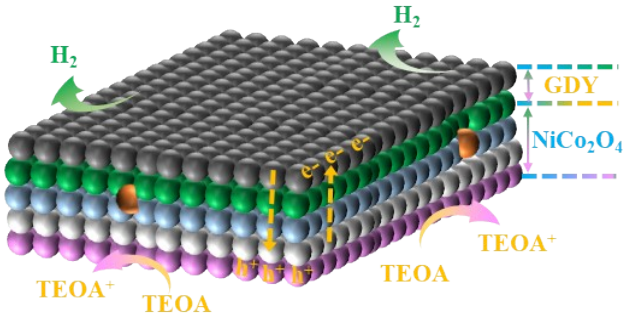

Fig. S9. An amorphous/crystalline system of $NiCo_2O_4$@GDY.

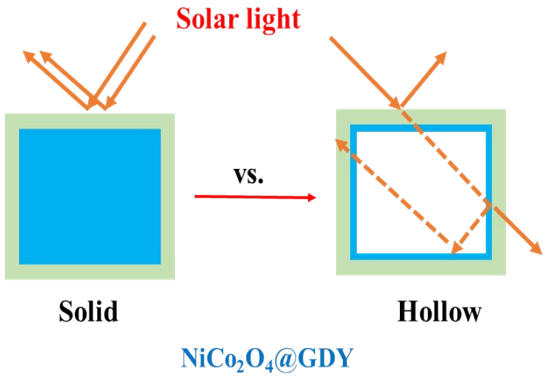

Fig. S10. Hollow structure of $NiCo_2O_4$ $NiCo_2O_4$@GDY.

Reference:

S1 C. Wang, X. Han, Q. Xu, Y. Sun, J. Arbiol, M. Ghazzal, J. Li, *J. Mater. Chem. A*, 2023, **11**, 3380-3387.

S2 Y. Zhang, H. Liu, M. Yang, S. Li, Z. Jin, *Appl. Mater. Today*, 2023, **31**, 101735.

S3 X. Yin, S. Luo, S. Tang, X. Lu, T. Lu, *Chin. J. Catal.*, 2021, **42**, 1379-1386.

S4 K. Yang, T. Liu, D. Xiang, Y. Li, Z. Jin, *Sep. Purif. Technol.*, 2022, **298**, 121564.

S5 J. Li, M. Li, H. Li, Z. Jin, *J. Mater. Chem. C*, 2022, **10**, 2181-2193.

S6 Z. Jin, H. Li and J. Li, *Chin. J. Catal.*, 2022, **42**, 303-315.

S7 Z. Jin, X. Wang, X. Hao, G. Wang, X. Guo, K. Wang, *2D Mater.*, 2022, **9**, 025014.

S8 Z. Jin, X. Jiang, Y. Liu, *Renew. Energy*, 2022, **201**, 854-863.